Available online at www.sciencedirect.com
SCIENCE DIRECT®
Journal of Power Sources 144 (2005) 83–93
JOURNAL OF POWER SOURCES
www.elsevier.com/locate/jpowsour

Systematic parameter estimation for PEM fuel cell models

Brian Carnes, Ned Djilali*

Institute for Integrated Energy Systems (IESVic), University of Victoria, Victoria, BC, Canada V6W 3P6

Received 7 October 2004; received in revised form 1 December 2004; accepted 1 December 2004
Available online 23 February 2005

Abstract

The problem of parameter estimation is considered for the case of mathematical models for polymer electrolyte membrane fuel cells (PEMFCs). An algorithm for nonlinear least squares constrained by partial differential equations is defined and applied to estimate effective membrane conductivity, exchange current densities and oxygen diffusion coefficients in a one-dimensional PEMFC model for transport in the principal direction of current flow. Experimental polarization curves are fitted for conventional and low current density PEMFCs. Use of adaptive mesh refinement is demonstrated to increase the computational efficiency.

Keywords: Parameter estimation; PEM fuel cell; Adaptive mesh refinement

1. Introduction

Mathematical models are now widely used to simulate the behavior of fuel cell devices. Such models are desirable because they can provide general trends as well as quantitative measures of relative changes in performance for the device as model parameters are varied. The models can also provide detailed, localized data that are frequently unavailable from experimental measurements within an operating cell.

However, the detailed data and parametric studies produced by computer simulations should not be accepted without appropriate validation with experimental data. This validation may include reduction of modeling error by comparing a chosen mathematical model to other potential models or reduction of parameter error by adjusting the parameters of the chosen model. In each case, the goal is to minimize the discrepancy between the computed simulation and the observable experimental data. Estimation of the model parameters is the focus of this study.

The problem of parameter estimation can be summarized in general terms as follows. Suppose that we have developed a mathematical model which takes the form of a system of partial differential equations (PDEs) for the solution variables, as well as a set of model parameters, both discrete (finite) or spatially distributed (infinite). Suppose also that certain experimental data are available, which we assume correspond to evaluations of various observable outputs of the solution variables. The problem is then to find an optimal set of parameter values that minimizes the error between the observed output functionals of the experimental data and those outputs calculated using the solution to the mathematical model.

In the case of fuel cells, while there have been some recent works which report local current density data using segmented current collectors [1], typically the experimental data are available only for global output quantities such as polarization curves, overall water balances, etc. Furthermore, these data are actually a set of measurements over a range of operating conditions as a parameter, such as the average current density, cell potential, relative humidity, etc. is varied. Therefore, the comparison between model and experiment can only be made globally using data that represent an average performance of the fuel cell. This point is particularly significant in the case of fuel cell stacks, where the local current, mass fluxes, temperature, etc. may vary significantly from the average measured data.

For the case of polymer electrolyte membrane fuel cells (PEMFCs), the mathematical model is chosen to represent various reaction and transport processes within a cell, such as

* Corresponding author. Tel.: +1 250 7216034; fax: +1 250 7216323.
E-mail addresses: carnes22@uvic.ca (B. Carnes); ndjilali@uvic.ca (N. Djilali).

0378-7753/$ – see front matter © 2005 Elsevier B.V. All rights reserved.
doi:10.1016/j.jpowsour.2004.12.024

convection–diffusion transport, electrochemical reaction and membrane water and proton transport. The solution variables can include fluid velocity and pressure, species composition, temperature, scalar potentials, etc. while the parameters may include the membrane conductivity, reference exchange current densities, electro-osmotic drag coefficient, etc. An additional motivation for parameter estimation is the lack of understanding of fundamental transport processes such as migration of protons and liquid water through the membrane, which can lead to semi-empirical models with unknown, sometimes nonphysical parameters, which must somehow be estimated.

Many mathematical models for PEMFCs have been described in the literature, ranging from one-dimensional models in the direction of current or gas flow [1–5] to two- and three-dimensional models [6–10]. However, most of these authors do not address the question of parameter estimation using a systematic approach. Thampan et al. [11] and Fimrite [12] performed parameter estimation for membrane conductivity submodels using curve fitting techniques. Suares and Hoo [13] estimated PEMFC model parameters for the model of Nguyen and White [4], such as exchange current density using an optimization approach. Berg et al. [1] estimate several parameters using a one-dimensional PEMFC model based on [4]. Recently, Guo et al. [14] have fitted cathode catalyst layer parameters such as porosities, reference current densities and effective diffusion coefficients using a one-dimensional cathode catalyst layer model.

In this work, we demonstrate the use of parameter estimation for a one-dimensional model for a PEMFC that accounts for conduction of protons and electrons, diffusion of oxygen and the electrochemical reactions. We present results on estimation of the effective membrane conductivity, effective volumetric exchange current densities in the cathode and anode catalyst layers, and effective oxygen diffusion coefficients in the gas diffusion and catalyst layers, paying special attention to the sensitivity coefficients, which indicate the significance of a parameter at each data point on the experimental polarization curve. The algorithm for parameter estimation is based on least squares minimization with constraints arising from the solution of a system of nonlinear PDEs, and is sufficiently general that it can be extended to multidimensional, transient models, or to include additional physical phenomena in the mathematical model. In addition, we study the effects of mesh refinement on the accuracy of the parameter estimation, including the use of locally refined meshes for greater efficiency and reliability.

The remainder of this work is organized as follows. We first describe our one-dimensional transport model for a PEMFC. Then we provide an algorithm for parameter estimation with PDE constraints based on a nonlinear least squares approach. Next, we present numerical results for estimating parameters using conventional PEMFC dimensions and data for regions with no mass transport limitations, as well as for an air-breathing PEMFC that is mass transport limited. We conclude with an example illustrating the effectiveness of using adaptive mesh refinement.

2. One-dimensional PEMFC model equations

In this section, we define a simple one-dimensional model for reaction and transport within a PEMFC. Since the principal axis of transport of current is in the direction normal to the membrane, we choose the x-axis in this direction, oriented from anode to cathode. A schematic of the PEMFC layers and dependent variables is shown in Fig. 1.

Conduction of electrons through the catalyst layers and gas diffusion layers (GDLs) is modeled using a solid electrical potential ϕ_e and conduction of the protons in the membrane and catalyst layers is modeled using an ionic potential ϕ_m. In the cathode side GDL and catalyst layer, we model the transport of oxygen using the oxygen mole fraction X_{O_2}. Conservation of charge and mass, combined with Ohm's law and Fick's law, yields the nonlinear boundary value problem: find $\{\phi_e, \phi_m, X_{O_2}\}$ such that

$$-\frac{d}{dx}\left(\sigma_e \frac{d}{dx}\phi_e\right) = j, \quad \text{GDLs and catalyst layers,} \tag{1a}$$

$$-\frac{d}{dx}\left(\sigma_m \frac{d}{dx}\phi_m\right) = -j, \quad \text{membrane and catalyst layers,} \tag{1b}$$

$$-\frac{d}{dx}\left(cD\frac{d}{dx}X_{O_2}\right) = -\frac{j}{4F}, \quad \text{cathode GDL and catalyst layer,} \tag{1c}$$

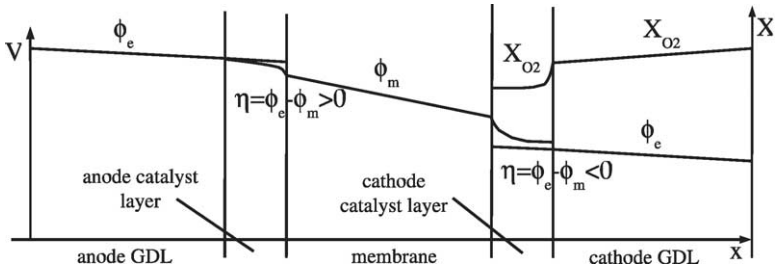

Fig. 1. Schematic of one-dimensional PEMFC model.

$$\eta \equiv \phi_e - \phi_m, \quad \text{overpotential in catalyst layers.} \tag{1d}$$

Here σ_e is the electrical conductivity, σ_m the ionic conductivity, c the molar concentration and D is the molecular diffusivity. The nonlinear reaction kinetics are given by a Butler–Volmer expression

$$j \equiv j_s\{\exp(\beta n f\eta) - \exp((\beta - 1)nf\eta)\}, \tag{2}$$

where j_s is the exchange current density with $s = a, c$ for anode and cathode, respectively, β the transfer coefficient, n the number of electrons transferred and $f \equiv F/RT$ is a factor depending on the Faraday constant F, ideal gas constant R and temperature T [15]. A common assumption [10] is that $\beta = 1/2$, in which case we can define $\alpha \equiv \beta n = -(\beta - 1)n$ and then

$$j \equiv j_s\{\exp(\alpha f\eta) - \exp(-\alpha f\eta)\} = j_s 2\sin h(\alpha f\eta). \tag{3}$$

In general, the transport of hydrogen in the anode GDL and consumption in the anode catalyst layer should be included in the model. However, in the context of fitting parameters using polarization curve data, the hydrogen mass transport limitations and resulting overpotential losses are likely to be dominated by ohmic, cathodic overpotential and oxygen limiting losses [6]. It is therefore reasonable to assume that hydrogen concentration is nearly constant, while oxygen concentration is expected to vary more widely. We make the assumption that the exchange current density is constant in the anode and first-order in the cathode

$$j_a = j_a^{\text{ref}}, \quad j_c = j_c^{\text{ref}}\left(\frac{c_{O_2}}{c_{O_2}^{\text{ref}}}\right) = j_c^{\text{ref}}\left(\frac{c}{c_{O_2}^{\text{ref}}}\right)X_{O_2}. \tag{4}$$

The boundary conditions are specified as follows:

- anode GDL boundary with the anode gas channel: $\phi_e = 0$;
- GDL/catalyst layer: zero ionic current or $-\sigma_m \frac{d}{dx}\phi_m = 0$;
- catalyst layer/membrane: zero electrical current or $-\sigma_e \frac{d}{dx}\phi_e = 0$;
- membrane/cathode catalyst layer: zero oxygen flux or $-cD\frac{d}{dx}X_{O_2} = 0$;
- cathode GDL boundary with cathode gas channel: total potential drop $\phi_e = -dV$ and reference oxygen mole fraction $X_{O_2} = X_{O_2}^{\text{ambient}}$.

For conventional PEMFCs with flow fields, $X_{O_2}^{\text{ambient}}$ will vary along the flow channels, and can be interpreted as an average value, while for ambient air-breathing PEMFCs, we can define $X_{O_2}^{\text{ambient}}$ using the ambient oxygen composition. In the fitting procedure later, we only consider the oxygen equation for ambient air-breathing PEMFCs.

We specify a given potential drop dV, solve the model equations, and then calculate the current density by computing the electrical current $I = -\sigma_e \frac{d}{dx}\phi_e$ evaluated at the cathode GDL boundary. The cell voltage is then computed to be $V = V_{oc} - dV$, where V_{oc} is the experimentally measured open circuit potential.

We now define a subset of parameters on which to apply the parameter estimation procedure of Section 3. These are the membrane ionic conductivity σ_{mem}, the cathode reference exchange current density j_c^{ref}, the anode reference exchange current density j_a^{ref}, and the oxygen diffusion coefficients D_{gdl} and D_{cat} in the cathode side GDL and catalyst layer, respectively. We will assume that all other parameters and dimensions are known, and will seek to estimate only these five parameters.

3. Algorithm for nonlinear least squares with PDE constraints

In this section, we briefly outline the nonlinear least squares (NLS) approach, introduce the concept of implicit least squares through PDE constraints, and give an algorithm for NLS with PDE constraints.

The Lagrangian approach to constrained optimization is well known (cf. [16,17]). As part of this work, an algorithm was developed by the authors based on extending the Lagrangian approach. This allows for elimination of the Lagrange multipliers, avoiding solution of a large coupled system for the parameters, solutions, and Lagrange multipliers. In exchange, we must solve additional linear equations for the sensitivity functions, but can sequentially solve a number of decoupled systems in order to compute each parameter update.

Suppose that we have M data pairs $\{(I_i, V_i)\}_{i=1}^M$ and a fitting function $I = I(\lambda; V)$ with N parameters $\lambda = \{\lambda_j\}_{j=1}^N$. For example, these may be taken as the current density I and cell voltage V from polarization curve data, as will be done in Section 4. We would like to choose the parameters λ in order to approximate the data at each data pair as:

$$I(\lambda; V_i) \approx I_i. \tag{5}$$

A common way to do this is to minimize a least squares functional

$$\mathcal{M}(\lambda) \equiv \frac{1}{2}||m||^2 = \frac{1}{2}\sum_{i=1}^{M}|m_i(\lambda)|^2,$$
$$m_i(\lambda) \equiv \omega_i(I(\lambda; V_i) - I_i), \tag{6}$$

using a NLS algorithm, where the m_i's are called the misfits. The constants ω_i can be chosen to produce a weighted data fit. For simplicity we take $\omega_i = 1$ throughout.

At a local minimum we must have $\nabla\mathcal{M} = (\nabla m)^T m = 0$, or

$$\sum_{i=1}^{M} m_i \frac{\partial m_i}{\partial \lambda_j} = 0, \tag{7}$$

which defines the set of solutions of the NLS problem. In order to solve (7), we can apply Newton–Raphson iteration. The system that we solve for the update $\delta\lambda$ at each iteration

takes the form $J\,\delta\lambda = r$, where

$$r_j \equiv -\sum_{i=1}^{M} m_i \frac{\partial m_i}{\partial \lambda_j},$$

$$J_{jk} \equiv -\frac{\partial r_j}{\partial \lambda_k} = \sum_{i=1}^{M} \left\{ \frac{\partial m_i}{\partial \lambda_j}\frac{\partial m_i}{\partial \lambda_k} + m_i \frac{\partial^2 m_i}{\partial \lambda_j \partial \lambda_k} \right\}. \tag{8}$$

If we assume each m_i is small, we can drop the second term and solve using the Gauss–Newton method, which takes the form $M\,\delta\lambda = r$, where

$$M_{jk} \equiv \sum_{i=1}^{M} \frac{\partial m_i}{\partial \lambda_j}\frac{\partial m_i}{\partial \lambda_k}. \tag{9}$$

One advantage to this approach is that we only need to calculate the first-order partial derivatives $\frac{\partial m_i}{\partial \lambda_j}$ and no second-order derivatives.

The partial derivatives $\frac{\partial m_i}{\partial \lambda_j}$ are often called the sensitivity coefficients, because they measure the sensitivity of the *i*th misfit to perturbations in the *j*th parameter. They are also important to the question of solvability of the NLS problem, which is also called the problem of *identifiability* (see for instance [16]). Invertibility of the matrix M is equivalent to the vectors $\alpha^j \equiv (\frac{\partial m_1}{\partial \lambda_j}, \ldots, \frac{\partial m_M}{\partial \lambda_j}) \in \mathbb{R}^M$ being linearly independent. If the vectors are nearly linearly dependent, then the NLS problem can be difficult to solve and may even fail to converge. Thus, before proceeding with any NLS problem, it is prudent to identify any linear dependence in the vectors α^j.

The NLS approach described above is adequate when we have an explicit expression of the form $I = I(\lambda; V)$. However, often we are interested in solving stationary or transient PDEs with specified input value V and postprocessing the solution to obtain the output value I, or vice versa. The parameters λ are then the parameters of the PDE, and the "function" $I = I(\lambda; V)$ is computed by solving the PDE.

In this case, we must modify the NLS approach to include the PDE constraints and to handle the implicitly defined output function. If we denote the differential operator that models the the PEMFC by $R = R(u, \lambda; V)$, then solutions $u = u(\lambda; V)$ are defined by solving:

$$R(u, \lambda; V) = 0, \tag{10}$$

for given values of λ and V. The output I, is calculated as a functional of the solution, in the form $I = I(u)$. We denote the residuals for each value V_i by $R^i(u, \lambda) \equiv R(u, \lambda; V_i)$ with corresponding solutions $u_i = u_i(\lambda)$.

The constrained parameter estimation problem can then be expressed as follows: find u and λ that minimizes the functional

$$\mathcal{M}(u) \equiv \frac{1}{2}||m||^2 = \frac{1}{2}\sum_{i=1}^{M} |m_i(u_i)|^2,$$

$$m_i(u_i) \equiv I(u_i) - I_i, \tag{11}$$

subject to the constraints

$$R^i(u_i, \lambda) = 0. \tag{12}$$

The main difference is that the misfit functional is now a function of the solution variable u rather than the parameter λ. The dependence of u on λ is implicit in the constraints. We will assume for simplicity that I is linear, so that $I'(u)v = I(v)$.

A standard approach to solving the constrained parameter estimation problem is to introduce Lagrange multipliers, one for each solution u_i, and solve a large coupled system [17]. It turns out that we can eliminate the Lagrange multipliers and solve the constrained parameter estimation problem using a slightly modified form of the Gauss–Newton iteration in (9), provided that we can calculate the partial derivatives $\frac{\partial m_i}{\partial \lambda_j}$ and the components m_i. Using the chain rule, we can calculate

$$\frac{\partial m_i}{\partial \lambda_j} = \frac{\partial m_i}{\partial u_i}\frac{\partial u_i}{\partial \lambda_j} = I'(u_i)\frac{\partial u_i}{\partial \lambda_j} = I\left(\frac{\partial u_i}{\partial \lambda_j}\right). \tag{13}$$

Thus, if we could calculate the partial derivatives $\frac{\partial u_i}{\partial \lambda_j}$, we could evaluate $\frac{\partial m_i}{\partial \lambda_j}$. To see how to obtain these functions, we differentiate each PDE w.r.t. λ_j to obtain:

$$\frac{\partial R^i}{\partial u_i}\frac{\partial u_i}{\partial \lambda_j} + \frac{\partial R^i}{\partial \lambda_j} = 0. \tag{14}$$

Thus, by solving the auxiliary equations:

$$\frac{\partial R^i}{\partial u_i} w_{ij} = -\frac{\partial R^i}{\partial \lambda_j}, \tag{15}$$

we obtain $w_{ij} = \frac{\partial u_i}{\partial \lambda_j}$ and thus $\frac{\partial m_i}{\partial \lambda_j} = I(w_{ij})$.

We now define an algorithm for parameter estimation with PDE constraints shown in the box below.

Because the system in step (2) involves summation over the data index i, we can perform each iteration of the algorithm, which consists of steps (1–3), by looping over i and then j. Practically speaking, this means that we need only form and store the Jacobian matrix associated with the differential operator $\frac{\partial R^i}{\partial u_i}$ once for each index i in step (1) of each iteration. The linear systems can be solved by an LU factorization of the Jacobian matrix or else an iterative solver can be applied. The finite dimensional approximate solution vectors associated with δu_i and w_{ij} are stored for the entire iteration for use in step (3). Thus, the cost of each iteration of the algorithm is the same as solving $N(M + 1)$ Jacobian systems. The additional solution of the Gauss–Newton system in step (2) is then negligible. The result is the simultaneous calculation of the optimal parameters λ_j, the corresponding solutions u_i, the misfit values m_i, and the sensitivity coefficients $\frac{\partial m_i}{\partial \lambda_j}$.

This algorithm can be implemented in any computer code which allows access to the Jacobian matrix and residual vector and the linear algebra solver. If the partial derivatives $\frac{\partial R^i}{\partial \lambda_j}$ cannot be calculated explicitly, we may approximate them

Algorithm for NLS with PDE constraints
Initialize u_i for initial λ by solving $R^i(u_i, \lambda) = 0$.
Compute updates δu_i and $\delta\lambda_j$ as follows:
for $n = 1, 2, \ldots$ **do**

(1) Compute $m_i = I(u_i) - I_i$. Solve for initial δu_i and functions w_{ij}

$$\frac{\partial R^i}{\partial u_i}\delta u_i = -R^i \text{ (Newton–Raphson iteration).} \quad (16a)$$

$$\frac{\partial R^i}{\partial u_i} w_{ij} = -\frac{\partial R^i}{\partial \lambda_j}. \quad (16b)$$

(2) Solve $M\,\delta\lambda = r$ using modified Gauss–Newton iteration

$$r_j \equiv -\sum_{i=1}^{M}\{m_i + I(\delta u_i)\}I(w_{ij}), \quad (17a)$$

$$M_{jk} \equiv \sum_{i=1}^{M} I(w_{ij})I(w_{ik}). \quad (17b)$$

(3) Update δu_i using correction for λ

$$\delta u_i += \sum_{j=1}^{N} w_{ij}\delta\lambda_j. \quad (18)$$

Update $u_i += \delta u_i$ and $\lambda_j += \delta\lambda_j$, possibly with step size control.

end for

using the finite difference approximation:

$$\frac{\partial R^i}{\partial \lambda_j} \approx \frac{1}{\varepsilon}[R^i(u_i, \lambda + \varepsilon e_j) - R^i(u_i, \lambda)], \quad (19)$$

where e_j is the jth coordinate vector and $\varepsilon \ll 1$. If the code does not permit access to the Jacobian matrix, then we may directly approximate the partial derivatives $\frac{\partial m_i}{\partial \lambda_j}$ using:

$$\frac{\partial m_i}{\partial \lambda_j} \approx \frac{1}{\varepsilon}\left[m_i(u_i(\lambda + \varepsilon e_j)) - m_i(u_i(\lambda))\right], \quad (20)$$

where $u_i(\lambda)$ is the solution calculated at the parameter value λ.

We now apply the parameter estimation algorithm to our PEMFC model equations.

4. Application to the PEMFC model equations

The solution to the differential equations is approximated at each step of the parameter estimation algorithm by a standard Galerkin finite element method using piecewise linear basis functions. We begin with an initial coarse grid and apply the iterative algorithm, which usually converges in about four to eight iterations, to solve for approximate solutions u_{ih} and parameters λ_{jh}. Then we refine the grid and project the current approximate solutions onto the fine grid. Using the projected solutions as the initial guess we apply the iterative algorithm to obtain new approximate solutions and parameters. After sufficient levels of mesh refinement, the parameters tend to converge to a mesh-independent value, which we take as the final estimated parameter value.

The mesh refinement can be uniform, meaning that all cells are refined, or adaptive, meaning that we selectively refine cells based on a local error indicator function. Our computer code reports the values of the parameters calculated at each iteration for each mesh, which reveals the convergence of the parameter estimation algorithm on each individual mesh, as well as the convergence of the finite element approximation to the parameters.

We consider data from two different PEMFCs, which are shown in Fig. 2. The first data set is for a conventional PEMFC design using polarization data reported by Ticianelli et al. [18], while the second is an air-breathing PEMFC yielding lower current densities. We also plot our best fitted polarization curves, corresponding to the simultaneous fitting of σ_{mem} and j_c for the conventional PEMFC and to σ_{mem}, D_{cat}, and D_{gdl} for the low current density PEMFC.

In the parameter estimation procedure, we can choose to fit parameters individually, or simultaneously. While the former approach is numerically more reliable, it may not represent the coupling between the parameters. Therefore, the latter approach is preferred based on physical grounds. We choose to perform both approaches, in order to demonstrate the variation in the fit of the parameters. When a great deal of variation of a fitted parameter is seen using different combinations, this can be an indication that there is strong coupling between the parameters. In this case the data can be fit by multiple sets of parameters, and the model may be need to be revised.

4.1. Conventional PEMFC

We first fit our one-dimensional PEMFC model to the conventional PEMFC polarization curve.

4.1.1. Initial parameters

We take the physical dimensions of each layer and initial transport and reaction properties from Berning et al. [6], which we summarize in Table 1. The experimental data are from Ticianelli et al. [18] and takes the form of a curve fit

$$V = V_0 - b\,\log\left(\frac{I}{I_0}\right) - R\,I, \quad (21)$$

with parameter values $V_0 = 0.935\,\text{V}$, $b = 0.065\,\text{V}$, $I_0 = 1\,\text{mA cm}^{-2}$, and $R = 0.39\,\text{cm}^2\,\text{S}^{-1}$. The electrode is produced with a catalyst loading of $0.35\,\text{mg Pt cm}^{-2}$ with 4%

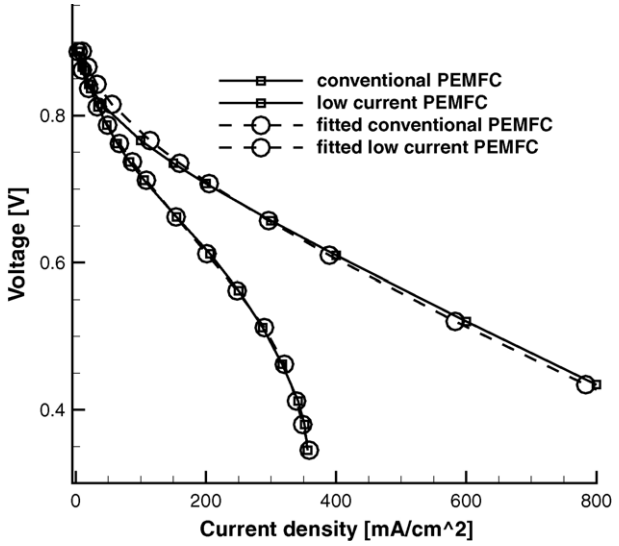

Fig. 2. Experimental and fitted polarization curves for conventional and low current PEMFC designs.

Nafion, the membrane is Nafion 117, and $V_{oc} = 0.935$. The PEMFC is operating on humidified hydrogen/air at pressures of 3/5 atm at 80 °C. Because the data are fitted to lower current density data, mass transport limitations are not significant. Therefore, we do not include the oxygen transport equation, assuming that the oxygen concentration is at the reference value. We seek to fit the parameters σ_{mem}, j_c, and j_a (dropping the superscript on j_s^{ref}).

For fully humidified Nafion 117, we expect $\sigma_{mem} \approx 8\,S\,m^{-1}$ from experimental measurements of the protonic conductivity of Nafion. We choose the initial value of $\sigma_{mem} = 6\,S\,m^{-1}$ following [6]. The exchange current densities are typically available as surface reaction rates; for example, in [6] they use values of $j_a = 6.0e{+}3\,A\,m^{-2}$ and $j_c = 4.4e{-}3\,A\,m^{-2}$. In order to derive effective volumetric exchange current densities, we must multiply by a correction factor that has units of $1\,m^{-1}$. Ideally this factor should account for the surface:volume ratio, the porosity of the catalyst layer, as well as the amount of Nafion and Pt applied when the catalyst layer was formed. We take our initial guess for the effective volumetric exchange current densities as $j_a = 1e{+}9\,A\,m^{-3}$ and $j_c = 2e{+}6\,A\,m^{-3}$.

Table 1
Initial physical transport and reaction parameters for conventional PEMFC

	Anode		Membrane	Cathode	
	Gas diff. layer	Cat. layer		Cat. layer	Gas diff. layer
Thickness, l (μm)	260	28	230	28	260
σ_e ($S\,m^{-1}$)	6000	6000	0	6000	6000
σ_m ($S\,m^{-1}$)	0	0.6	6	0.6	0
j_s ($A\,m^{-3}$)		1e+9		2e+6	
α		0.5		1.0	

We present in Fig. 3 the dimensionless sensitivity coefficients $\frac{\partial m_i}{\partial \lambda_j}$ for all three parameters, calculated at the initial values. Because of the near linear dependence of the sensitivity coefficients for σ_{mem} and j_a, we expect that these parameters may be coupled.

Another interesting observation to make about Fig. 3 is the variation in sensitivity as the average current density I is varied. While the sensitivity coefficients for σ_m and j_a remain fairly constant, the sensitivity coefficients for j_c are largest for small I, and decrease exponentially as I increases. This can be explained by the difference in the type of voltage losses. For the membrane, the ohmic loss is a linear function of the current with constant sensitivity to the conductivity, while for the cathode electrochemical reaction, the loss is a logarithmic function of the current with decreasing sensitivity to the reaction rate as I increases. By linearizing the anode reaction rate, it can be shown that the anode loss is also a linear function of the current, and thus, behaves as the membrane conductivity.

In many studies, the catalyst layers are modeled as thin interfaces or using a constant overpotential. In Fig. 4 we plot the overpotential η in the anode and cathode catalyst layers for the initial parameter values and varying current densities in order to illustrate the effect of solving a one-dimensional model for behavior that cannot be modeled using a reduced model. The maximal absolute values of η occurs along the membrane–catalyst layer interfaces, where the rate function has its largest absolute value. The larger rate constant at the anode results in faster kinetics and a smaller reaction region near the interface. We do not plot the solutions elsewhere, since ϕ_m varies linearly within the membrane, and ϕ_e is nearly constant in the GDLs.

4.1.2. Estimated parameters

We now estimate the parameters using our parameter estimation algorithm. We first compare the results obtained by

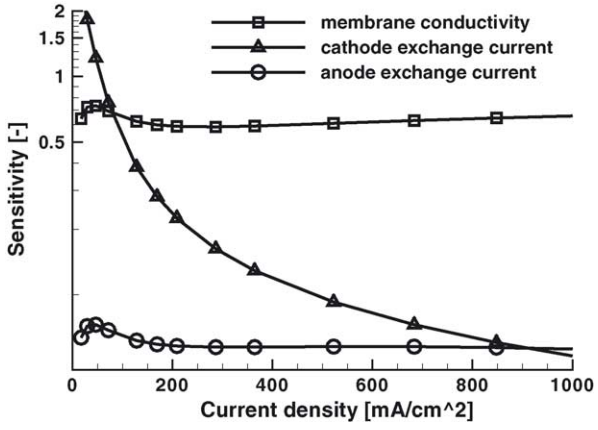

Fig. 3. Initial dimensionless sensitivity coefficients for conventional PEMFC.

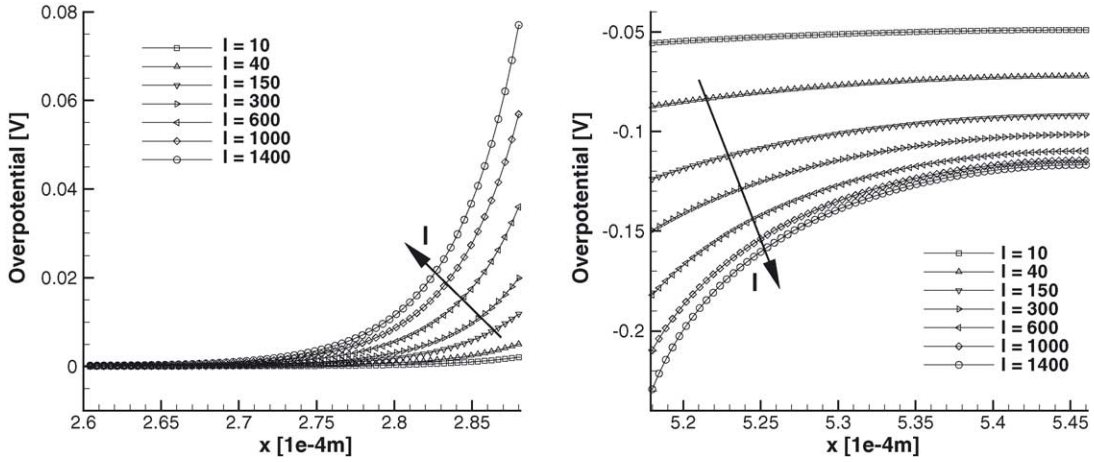

Fig. 4. Initial overpotential in anode (left) and cathode (right). I is given in units of mA cm^{-2}.

Table 2
Estimated parameters on fine grids for conventional PEMFC using different combinations of fitted parameters

	σ_{mem} (S m^{-1})	j_c (A m^{-3})	j_a (A m^{-3})
Initial	6	2e+6	1e+9
Fitted	7.67	–	–
	–	9.79e+5	–
	(7.67)	–	1.43e+9
	8.29	2.50e+6	–
	9.24	–	9.60e+8
	(7.67)	2.66e+6	9.02e+8

Values in parenthesis were fixed but chosen different from the initial guesses.

estimating each parameter separately, and then using combinations of parameters. The converged values are reported in Table 2.

Convergence of the estimated values for σ_{mem} using uniform mesh refinement is shown in Fig. 5. We can see convergence of the parameter estimation algorithm on each grid to a value λ_{jh}, as well as convergence of the values λ_{jh} as the mesh is refined. When we fit σ_{mem} or both σ_{mem}, j_c, the value is close to the fully humidified conductivity of 8 S m^{-1} for Nafion 117. However, fitting with both σ_{mem}, j_a yields a higher value of σ_{mem} by fitting a lower value of j_a.

We saw in Fig. 3 that the sensitivity of the current density I to j_c decreases dramatically as I increases. When a sensitivity coefficient is small, the term in (7) multiplied by the coefficient will also be small, and thus can be neglected. Therefore we choose to estimate j_c using current density only in the range of $I < 300$ mA cm^{-2}, where the sensitivity is largest. Inclusion of j_c is thus key to fitting low values of I, whereas inclusion of σ_{mem} is required for the entire range of I. This is consistent with the dominance of activation losses at low current densities and of ohmic losses at higher current densities, and explains why the best fittings are obtained using the combinations $\{\sigma_{mem}, j_c\}$ and $\{j_c, j_a\}$ (with the fitted σ_{mem} value).

Table 3
Initial physical transport and reaction parameters for a low current PEMFC

	Anode		Membrane	Cathode	
	Gas diff. layer	Cat. layer		Cat. layer	Gas diff. layer
Thickness, l (μm)	130	20	60	20	130
σ_e (S m^{-1})	100	100	0	100	100
σ_m (S m^{-1})	0	0.2	2	0.2	0
D_{O_2} (m^2 s^{-1})	0	0	0	3e−7	3e−6
j_s (A m^{-3})		1e+9		2e+6	
α		0.5		1.5	

4.2. Low current density PEMFC

We now fit our one-dimensional PEMFC model to the low current density PEMFC polarization curve.

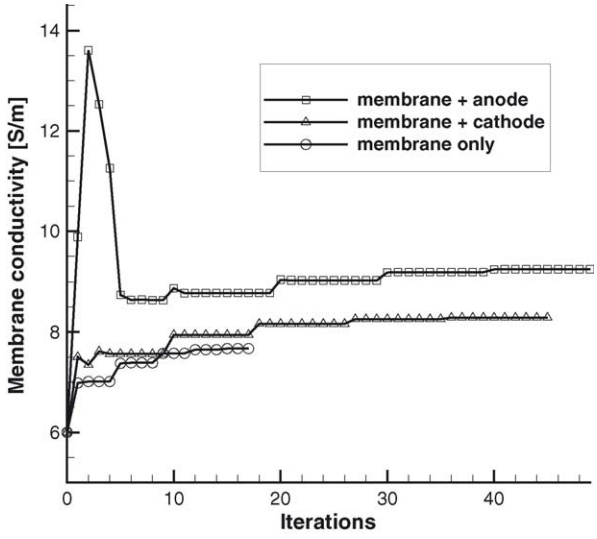

Fig. 5. Convergence of σ_{mem} for various parameter combinations.

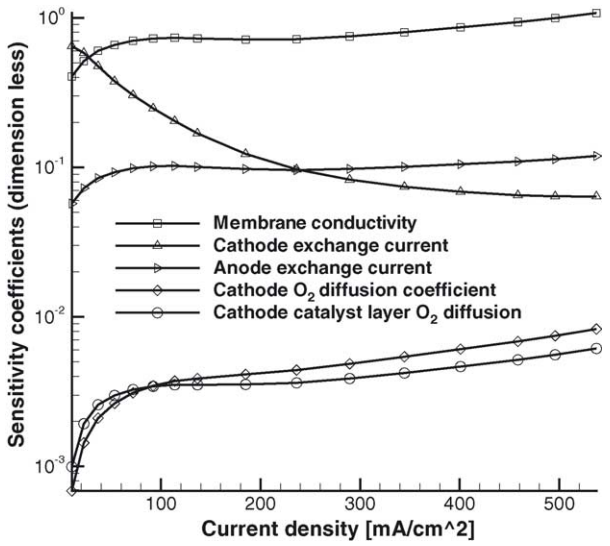

Fig. 6. Initial dimensionless sensitivity coefficients for a low current PEMFC.

4.2.1. Initial parameters

We adjust the dimensions and parameters for an air-breathing PEMFC which exhibits mass transport limitations at relatively low current densities as shown in Fig. 2. This cell uses a thinner membrane (Nafion 112) and thinner layers, which we summarize in Table 3. The temperature is now specified as 60 °C, $V_{oc} = 0.912$, and the ambient oxygen mole fraction is specified as 0.21. Because of the reduced slope of the polarization curve, we begin with a lower value for the membrane conductivity. The oxygen diffusion coefficient in the GDL is reduced by an order of magnitude to account for the porosity and tortuosity of the diffusion layer; in the catalyst layer this parameter is reduced by another order of magnitude to model additional resistance at reaction sites (see Fig. 6 for initial sensitivites).

4.2.2. Estimated parameters

We now apply the parameter estimation to the data for the low current PEMFC design. The converged estimated parameters are shown in Table 4.

The fitting of the parameters σ_{mem}, j_a, and j_c is performed using only data with $I < 200\,mA\,cm^{-2}$ and is similar to the case of the conventional fuel cell (see first section of fitted parameters in Table 4). However, the fitted membrane conductivity is now closer to $1\,S\,m^{-1}$, which corresponds to partially humidified operating conditions. In addition, the fitted cathode rate j_c is an order of magnitude lower than the initial value, which is caused by using the effective value of $2e{-}1\,S\,m^{-1}$ for the effective membrane conductivity in the catalyst layers.

We next fit the effective oxygen diffusion coefficients D_{gdl} and D_{cat} (second section of fitted parameters in Table 4) for the large current data ($I > 200\,mA\,cm^{-2}$) using the fitted σ_{mem}, j_a, and j_c values. The data can be fitted by reducing either D_{gdl} or D_{cat} by an order of magnitude, representing an additional mass transport resistance, such as liquid water flooding. We can also fit the diffusion coefficients, individually or simultaneously, along with σ_{mem}, over the entire polarization curve, using the fitted values for j_a and j_c (third section of fitted parameters in Table 4). We plot in Fig. 7 the oxygen profiles in the cathode catalyst layer for different current densities and parameter fittings. Fitting D_{gdl} results in a nearly constant, low oxygen concentration in the catalyst layer, while fitting D_{cat} results in a steep gradient in oxygen concentration in the catalyst layer. Simultaneous fitting lies somewhere in between, and distributes the mass transfer resistance between the GDL and the catalyst layer.

While simultaneous fitting provides the best possible data fit over the entire curve, all three fits are similarly good. The problem lies not in the parameter estimation procedure, but in the choice of the mathematical model. In order to fit the drop in current density of the data using the oxygen equation, we must add a certain amount of resistance to mass transport, in the form of reduced diffusion coefficients D_{gdl} and D_{cat}. The fairly small diffusion coefficients required to obtain a good fit (two to three orders of magnitude smaller than for pure gas mixtures), suggest that a macrohomogeneous mass transport resistance model may be inadequate to

Table 4
Estimated parameters for fine grids for low current PEMFC using different combinations of fitted parameters

	σ_{mem} ($S\,m^{-1}$)	j_c ($A\,m^{-3}$)	j_a ($A\,m^{-3}$)	D_{gdl} ($m^2\,s^{-1}$)	D_{cat} ($m^2\,s^{-1}$)
Initial	2	2e+6	1e+9	3e−6	3e−7
Fitted	0.715	–	–	–	–
	–	3.71e+5	–	–	–
	1.02	3.41e+5	–	–	–
	–	–	8.27e+7	–	–
	(1.02)	(3.41e+5)	1.03e+9	–	–
Fitted	(1.02)	(3.41e+5)	(1.03e+9)	1.66e−7	–
	(1.02)	(3.41e+5)	(1.03e+9)	–	1.89e−8
Fitted	1.10	(3.41e+5)	(1.03e+9)	1.63e−7	–
	1.16	(3.41e+5)	(1.03e+9)	–	1.76e−8
	1.15	(3.41e+5)	(1.03e+9)	5.27e−7	2.38e−8

Values in parenthesis were fixed but chosen different from the initial guesses.

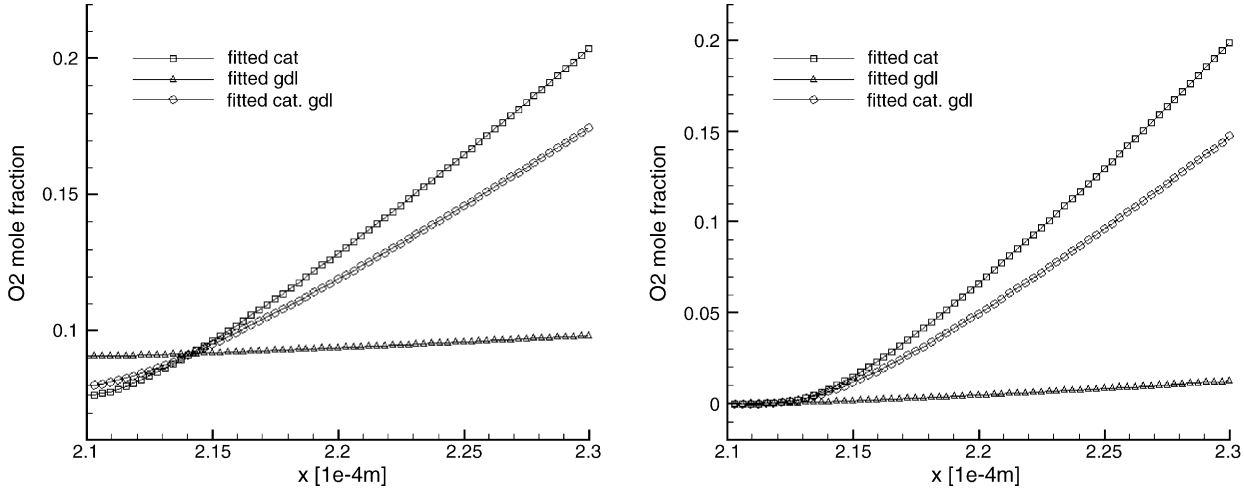

Fig. 7. Oxygen mole fraction profiles in the cathode catalyst layers obtained by fitting σ_{mem}, D_{cat} and D_{gdl} for $I = 317\,\text{mA cm}^{-2}$ (left) and $I = 356\,\text{mA cm}^{-2}$ (right).

describe the current losses, and an improved model should be sought.

Finally, we note that for large current densities where the model predicts severe oxygen depletion, the reaction rate can even develop an interior maximum within the catalyst layer, instead of along the membrane/catalyst layer interface, as seen in Fig. 8.

4.3. Adaptive mesh refinement

In this section, we demonstrate the use of adaptive mesh refinement (AMR) to increase the computational efficiency of the parameter estimation algorithm. Here instead of refining all elements of the mesh to obtain the next finer mesh, we choose only a subset of elements for refinement. To do this we need an error indicator function that associates a number with each element of the mesh, which represents an element contribution to the global error. For simplicity we choose an error indicator based on the jump in the flux $-au'$ of a scalar u between adjacent elements, defined on an element interface x by:

$$J_x \equiv -a(x^-)u'(x^-) + a(x^+)u'(x^+), \tag{22}$$

where the minuses (pluses) denote left (right) limits. For an element $K = (a, b)$, the local element error indicator is then defined by:

$$e_K^2 \equiv \sum \frac{b-a}{24}(|J_a|^2 + |J_b|^2), \tag{23}$$

where the summation is over all solution components $\{\phi_e, \phi_m, X_{O_2}\}$ and over all data points (I_i, V_i).

We now illustrate the effectiveness on the estimation of membrane conductivity σ_{mem} for the conventional PEMFC data. For the AMR, we sort the elements by their error indicator values and choose to refine those elements in the top 20% while coarsening those elements in the bottom 2%. An element is refined by inserting a new node at the element midpoint, while a pair of adjacent elements are coarsened by removing the common node. The solution on the original mesh is interpolated onto the new mesh as the new initial solution guess (for implementation see [19] or for general information on AMR see [20]). In Fig. 9 we plot the error indicator values in the catalyst layers, where the error indicators take on the largest values. We can clearly see that the AMR refines the mesh in order to equally distribute the local error indicator values, resulting in meshes with element sizes varying over several orders of magnitude. The result is that even with a simple error indicator we can reduce the number of degrees of freedom necessary to produce a reasonable parameter estimate, resulting in a more efficient computation.

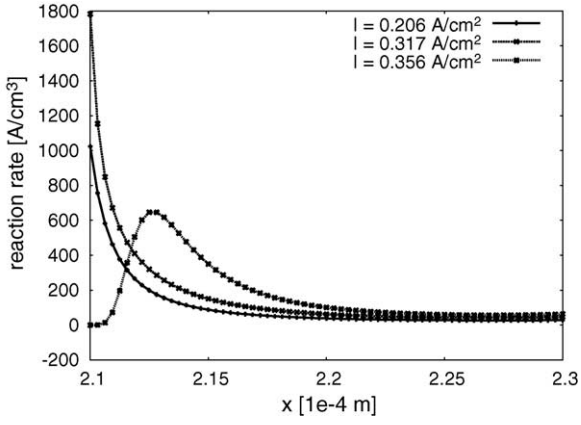

Fig. 8. Cathode reaction rates with oxygen limited kinetics.

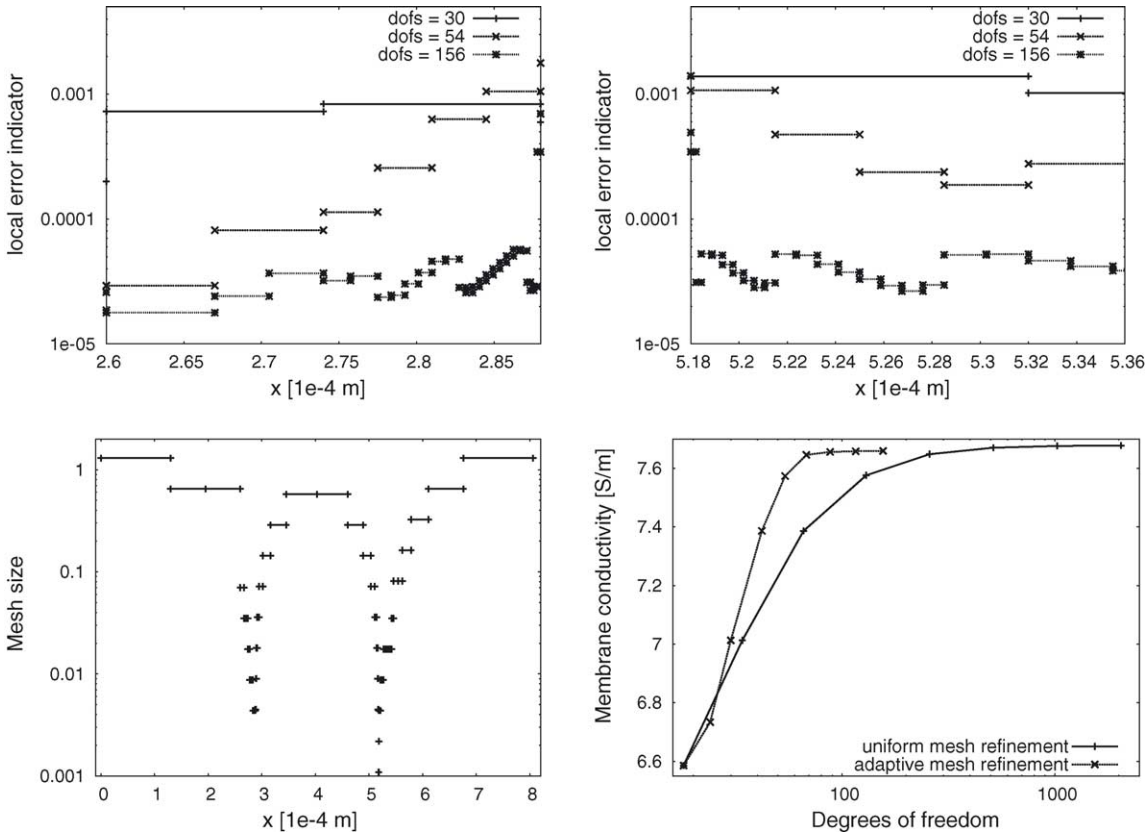

Fig. 9. Local error indicators used for adaptive mesh refinement in the anode (top left) and cathode (top right) catalyst layers. Final mesh size distribution (bottom left) and convergence of membrane conductivity (bottom right).

5. Conclusions

In this study, we have presented an algorithm for estimation of PEMFC model parameters using a constrained nonlinear least squares algorithm. Estimation of five model parameters in a simple one-dimensional electrochemistry model using two different experimental polarization curves has been demonstrated using this procedure. The potential for further enhancing the algorithm by integrating it with mesh refinement was demonstrated using an example showing the greater efficiency and reliability obtained from using initial guesses computed on coarse grids, as well as locally refined meshes.

This work naturally suggests potential additional research, including attempting parameter estimation for more complex PEMFC model equations, two- and three-dimensional simulations, as well as transient calculations. A key point is the need for additional data besides polarization curves, such as local data along the channel of operating cells, net water transfer balances from anode to cathode, or transient polarization curve data.

Acknowledgments

This work was supported in part by the Natural Sciences and Engineering Research Council of Canada and by the MITACS Network of Centres of Excellence.

References

[1] P. Berg, K. Promislow, J. St. Pierre, J. Stumper, Water management in pem fuel cells, J. Electrochem. Soc. 37 (3) (2004) 341–353.
[2] D.M. Bernardi, M.W. Verbrugge, Mathematical model of a gas diffusion electrode bonded to a polymer electrolyte, AIChE J. 37 (8) (1991) 1151–1163.
[3] T. Fuller, J. Newman, Water and thermal management in solid–polymer–electrolyte fuel cells, J. Electrochem. Soc. 140 (5) (1993) 1218–1224.
[4] T.V. Nguyen, R.E. White, A water and heat exchange model for proton-exchange-membrane fuel cells, J. Electrochem. Soc. 140 (8) (1993) 2178–2186.
[5] T.E. Springer, T.A. Zawodzinski, S. Gottesfeld, Polymer electrolyte fuel cell model, J. Electrochem. Soc. 138 (8) (1991) 2334–2342.
[6] T. Berning, D.M. Lu, N. Djilali, Three-dimensional computational analysis of transport phenomena in a pem fuel cell, J. Power Sources 106 (2002) 284–294.
[7] J.S. Yi, T.V. Nguyen, Multicomponent transport in porous electrodes of proton exchange membrane fuel cells using the interdigitated gas distributors, J. Electrochem. Soc. 146 (1) (1999) 38–45.
[8] S. Um, C.-Y. Wang, K.S. Chen, Computational fluid dynamics modeling of proton exchange membrane fuel cells, J. Electrochem. Soc. 147 (12) (2000) 4485–4493.
[9] K. Promislow, J. Stockie, Adiabatic relaxation of convective–diffusive gas transport in a porous fuel cell electrode, SIAM J. Appl. Math. 62 (1) (2001) 180–205.
[10] B.R. Sivertsen, N. Djilali, Cfd based modelling of proton exchange membrane fuel cells. J. Power Sources 141 (2005) 65–78.

[11] T. Thampan, S. Malhotra, H. Tang, R. Datta, Modeling of conductive transport in proton–exchange membranes for fuel cells, J. Electrochem. Soc. 147 (9) (2000) 3242–3250.
[12] J. Fimrite, Transport phenomena in polymer electrolyte membranes, MASc Thesis, IESVic, Univ. of Victoria (2004).
[13] G.E. Suares, K.A. Hoo, Parameter estimation of a proton-exchange membrane fuel cell using voltage–current data, Chem. Eng. Sci. 55 (12) (2000) 2237–2247.
[14] Q. Guo, V.A. Sethuraman, R.A. White, Parameter estimates for a pemfc cathode, J. Electrochem. Soc. 151 (7) (2004) 983–993.
[15] A.J. Bard, L.R. Faulkner, Electrochemical Methods: Fundamentals and Applications, Wiley, 2001.
[16] W.J.H. Stortelder, Parameter Estimation in Nonlinear Dynamic Systems. Number 124 in Tract. CWI, 1998.
[17] W. Bangerth, Adaptive finite element methods for the identification of distributed parameters in partial differential equations, Ph.D. Thesis, University of Heidelberg, 2002.
[18] E.A. Ticianelli, C.R. Derouin, A. Redondo, S. Srinivasan, Methods to advance technology of proton exchange membrane fuel cells, J. Electrochem. Soc. (1988).
[19] W. Bangerth, R. Hartmann, G. Kanschat, Deal.ii Differential Equations Analysis Library, Technical Report, University of Heidelberg http://www.dealii.org.
[20] G.F. Carey, Computational Grids: Generation, Adaptation and Solution Strategies, John Benjamins, 1997.